

Bone marrow-derived mononuclear cell therapy attenuates silica-induced lung fibrosis

Tatiana Maron-Gutierrez^{1,2}, Raquel C. Castiglione¹, Debora G. Xisto², Mariana G. Oliveira², Fernanda F. Cruz², Ramon Peçanha⁴, Humberto Carreira-Junior², Débora S. Ornellas², Milton O. Moraes⁴, Christina M. Takiya³, Patricia R.M. Rocco², Marcelo M. Morales¹

¹Laboratory of Cellular and Molecular Physiology, Federal University of Rio de Janeiro, Rio de Janeiro, Brazil

²Laboratory of Pulmonary Investigation, Carlos Chagas Filho Biophysics Institute, Federal University of Rio de Janeiro, Rio de Janeiro, Brazil

³Laboratory of Cellular Pathology, Biomedical Sciences Institute, Federal University of Rio de Janeiro, Rio de Janeiro, Brazil

⁴Leprosy Laboratory, Oswaldo Cruz Institute, FIOCRUZ, Rio de Janeiro, Brazil

CORRESPONDENCE

Marcelo Marcos Morales

Universidade Federal do Rio de Janeiro

Instituto de Biofísica Carlos Chagas Filho - C.C.S.

Laboratório de Fisiologia Celular e Molecular

Ilha do Fundão

21941-902 - Rio de Janeiro - RJ, Brazil

Tel.: +55 21 2562 6572; fax: +55 21 2280 8193

E-mail: mmorales@biof.ufrj.br

ABSTRACT

This study tests the hypothesis that bone marrow-derived mononuclear cell (BMDMC) therapy may reduce lung inflammation and fibrosis leading to an improvement in respiratory mechanics in a murine model of silicosis.

Fifty-two female C57BL/6 mice were randomly assigned into four groups. In SIL group, silica suspension (SiO₂; 20 mg/50 µl in saline) was intratracheally (i.t.) instilled and in C animals, saline (50 µl i.t.) was administered. At one hour, C and SIL groups were further randomized receiving BMDMC (2×10⁶, intravenously) (C-Cell and SIL-Cell) or saline (50 µl, i.v.) (C and SIL). BMDMC were obtained from male donor mice. At day 15, lung mechanics, histology, the presence of Y chromosome, interleukin (IL)-1β, IL-1α,

interleukin-1 receptor antagonist (IL-1RN), interleukin-1 receptor type 1 (IL-1R1), transforming growth factor (TGF)- β , and caspase-3 mRNA expressions in lung tissue were analysed.

In SIL-Cell group, the fraction area of granuloma, the number of macrophages, and collagen fibre content were reduced yielding improved lung mechanics. The presence of male donor cells in lung tissue was not confirmed using detection of Y chromosome DNA. Nevertheless, caspase-3, IL-1 β , IL-1 α , IL-1RN, and TGF- β mRNA expression diminished after cell therapy.

In conclusion, BMDMC acted on inflammatory and fibrogenic processes improving lung function through paracrine effects.

KEYWORDS: Collagen, elastance, macrophages, cell therapy

ABBREVIATIONS: BMDMC, bone marrow-derived mononuclear cells; C, control group; E_{st} , static elastance; GADPH, glyceraldehyde-3-phosphate dehydrogenase; IL-1 β , interleukin-1 β ; IL-1 α , interleukin-1 α ; IL-1RN, interleukin-1 receptor antagonist; IL-1R1, interleukin-1 receptor type 1; P_{el} , elastic recoil pressure; ΔP_1 , resistive pressure; ΔP_2 , viscoelastic pressure; ΔP_{tot} , total pressure; SIL, silica group; TGF- β , transforming growth factor- β ; V_T , tidal volume.

INTRODUCTION

Silicosis is a pneumoconiosis that involves formation of nodules and destruction of large areas of the lung leading to impaired gas-exchange and pulmonary function, which may result in respiratory failure. Despite extensive efforts, no available therapy has been shown to halt or efficiently reverse this disorder [1-3].

Adult bone marrow-derived cells (BMDC) act as progenitor cells in replacing and/or repairing injured tissues [4] in experimental models of fibrosis [5-7]. Recently, we analyzed the role of intratracheal instillation of BMDC in a model of silicosis and observed only a mild improvement in lung mechanics [8], which may be attributed to: (1) the pathogenesis of silicosis, (2) the timing of BMDC injection (early or late in the course of lung injury), and (3) the type of cell and route of administration. Therefore, we tested the hypothesis that early, intravenous and a single dose of bone marrow-derived mononuclear cells (BMDMC) may avoid mechanical changes in the lung in a murine model of silica-induced fibrosis. For this purpose, lung static elastance, resistive and viscoelastic pressures, histology, and inflammatory and fibrogenic mediators were measured 15 days after silica instillation.

METHODS

This study was approved by the Ethics Committee of the Carlos Chagas Filho Institute of Biophysics, Health Sciences Centre, Federal University of Rio de Janeiro. All animals received humane care in compliance with the *Principles of Laboratory Animal Care* formulated by the National Society for Medical Research and the *Guide for the Care and Use of Laboratory Animals* prepared by the National Academy of Sciences, USA.

Animal preparation and experimental protocol

Ninety-one C57BL/6 mice (72 females and 19 males, 20–25 g) were kept under specific pathogen-free conditions in the animal care facility of Laboratories of Pulmonary Investigation and Cellular and Molecular Physiology, Federal University of Rio de Janeiro. Thirty-two female mice were used to evaluate lung mechanics and histology, and mRNA expression of caspase-3, interleukin (IL)-1 β , IL-1 α , interleukin-1 receptor antagonist (IL-1RN), interleukin-1 receptor type 1 (IL-1R1) and transforming growth factor (TGF)- β , while Y chromosome DNA detection was performed in the remaining 40. All animals were randomly assigned to four groups. In SIL group, mice received intratracheal (i.t.) injection of 20 mg of silica crystals (SiO₂, particle size: 80% between 1 and 5 μ m; Sigma Chemical, St. Louis, MO) suspended in saline solution (total volume = 50 μ l), while saline (50 μ l i.t.) was instilled in control group (C). One hour after saline or silica administration, BMDMC from male mice (2×10^6 cells/50 μ l of saline) were injected intravenously (i.v.) (C-Cell and SIL-Cell groups).

Extraction of BMDMCs

Bone marrow cells from male C57BL/6 mice ($n=14$, 20–25 g) were aspirated from the femur and tibia by flushing the bone marrow cavity with Dulbecco's modified Eagle's medium (DMEM) (Life Technologies®, Grand Island, NY, USA). After a homogeneous cell suspension was achieved, the cells were centrifuged ($400 \times g$ for 10 min), re-suspended in DMEM and added to Ficoll-Hypaque (Histopaque 1083, Sigma Chemical Co., St. Louis, MO, USA), and again centrifuged and supplemented with sterile phosphate-buffered saline

(PBS). Cells were counted in a Neubauer chamber with Trypan Blue for evaluation of viability. Cell characterization was performed by flow cytometry using specific antibodies.

Lung mechanics

Fifteen days after administration of saline or silica, the animals were sedated (diazepam 1 mg i.p.), anesthetized (thiopental sodium 20 mg/kg i.p.), tracheotomized, paralyzed (vecuronium bromide, 0.005 mg/kg i.v.), and ventilated with a constant flow ventilator (Samay VR15; Universidad de la Republica, Montevideo, Uruguay) with the following parameters: frequency of 100 breaths/min, tidal volume (V_T) of 0.2 ml, and fraction of inspired oxygen of 0.21. The anterior chest wall was surgically removed and a positive end-expiratory pressure of 2 cmH₂O applied. After a 10-min ventilation period, lung mechanics were computed and at the end of the experiments (approximately 30 min), lungs were prepared for histology.

Lung static elastance (E_{st}), resistive (ΔP_1) and viscoelastic (ΔP_2) pressures were measured by the end-inflation occlusion method [9]. All data were analyzed using ANADAT data analysis software (RHT-InfoData, Inc., Montreal, Quebec, Canada).

Histology

A laparotomy was done immediately after the determination of lung mechanics and heparin (1000 IU) was injected intravenously in the vena cava. The trachea was clamped at end-expiration, and the abdominal aorta and vena cava were sectioned, yielding a massive haemorrhage that quickly killed the animals. The right lung was fixed with 10% buffered formaldehyde solution and paraffin embedded. Four-micrometre-thick slices (3/lung) were cut and stained with haematoxylin–eosin.

Lung morphometric analysis was performed using an integrating eyepiece with a coherent system consisting of a grid with 100 points and 50 lines (known length) coupled to a conventional light microscope (Olympus BX51, Olympus Latin America-Inc., Brazil). The area fraction of granuloma was determined by the point-counting technique across 20 random non-coincident microscopic fields at a magnification of $\times 200$. Polymorphonuclear, mononuclear and total cells in lung parenchyma and granuloma were evaluated at $\times 1000$ magnification and determined by the point-counting technique [10].

Collagen fibres (picrosirius method) were quantified in both alveolar septa and granuloma [11]. Immunohistochemistry was performed with the conventional avidin-biotin-peroxidase histochemical technique using a goat anti-rat biotinylated antibody (Vector Laboratories, Burlingame, CA, USA, cat. BA-4001) for biotinylated *Bandeiraea Simplicifolia* lectin 1 (BSL-1; Vector Laboratories, cat. B1205) which labels macrophages [12-13]. In each slide, 15 different microscopic fields were randomly selected and quantification ($\times 200$ magnification) was carried out with the aid of a digital camera (Evolution, Media Cybernetics, Silver Spring, MD, USA) coupled to a light microscope (Eclipse 400, Nikon, Tokyo, Japan). High quality (2048 \times 1536 pixels) images were obtained using the Image Pro Plus 4.5.1 software (Media Cybernetics, Silver Springs, MD, USA). The thresholds for collagen fibres were established after the contrast was enhanced up to a point at which the fibres were easily identified as birefringent bands. The area occupied by collagen fibres was determined by digital densitometric recognition. Bronchi and blood vessels were carefully avoided during the measurements. The area occupied by fibres was divided by tissue area and expressed as fraction area of collagen fibre. Positive cells (macrophages) were counted

and divided by lung parenchyma and granuloma area and expressed as fraction area of macrophages.

Y Chromosome DNA detection

Quantification of murine Y chromosome in lung tissue was achieved by quantitative real-time polymerase chain reaction (PCR) at days 1, 3, 7 and 15. Briefly, DNA was purified in a 600- μ l solution of 0.2% sodium dodecyl sulfate (SDS)/proteinase K (300 μ g/ml), extracted with an equal volume of phenol/chloroform/isoamyl alcohol. After centrifugation, the aqueous phase was transferred to a new tube, DNA was precipitated with 2 volumes of ethanol 100%. DNA was resuspended and quantified in a nanodrop spectrophotometer. Five nanograms of DNA were used in a real-time PCR reaction with the SYBR Green detection kit run in a 7000-sequence detection system thermocycler according to the manufacturer's instructions (Applied Biosystems, Foster City, CA). The following PCR primers were used: forward 5'-TCA TCG GAG GGC TAA AGT G-3' and reverse 5'-CAA CCT TCT GCA GTG GGA C-3'. Primer sequences were defined using primer3 software based on the *Mus musculus* sex-determining region of the Chr Y (Sry) gene (GenBank accession number: NM_011564; National Institutes of Health, NIH, Bethesda, MD, USA). These primers amplify an 88 bp product. The relative amount of total DNA was calculated as a ratio ($2^{-\Delta C_t}$) of Sry and glyceraldehyde-3-phosphate dehydrogenase (GAPDH). Primers for GAPDH: forward 5'-CCA CCA ACT GCT TAG CCC-3' and reverse 5'-GAC ACC TAC AAA GAA GGG TCC A-3', 145 bp [8].

Expression of caspase-3, IL-1 β , IL-1 α , IL-1RN, IL-1R1 and TGF- β

Quantitative real-time reverse transcription (RT) PCR was performed to measure the relative levels of expression of inflammatory and fibrogenic mediators. Central slices of left lung were cut, collected in cryotubes, quick-frozen by immersion in liquid nitrogen and stored at -70°C . Total RNA was extracted from the frozen tissues using the Trizol reagent (Invitrogen, Carlsbad, CA) according to the manufacturer's recommendations. RNA concentration was measured by spectrophotometry in Nanodrop® ND-1000. First-strand cDNA was synthesized from total RNA using a M-MLV Reverse Transcriptase Kit (Invitrogen, Carlsbad, CA). PCR primers for the target gene were purchased from Invitrogen. Relative mRNA levels were measured with a SYBR Green detection system using ABI 7500 Real-Time PCR (Applied Biosystems). All samples were measured in triplicate. The relative amounts of caspase-3, IL-1 β , and TGF- β expression were calculated as a ratio ($2^{-\Delta C_t}$) of the study gene and the control gene (GAPDH). Primers used and PCR product size were: caspase-3, forward 5'-TAC CGG TGG AGG CTG ACT-3' and reverse 5'-GCT GCA AAG GGA CTG GAT-3', 104 bp; IL-1 β , forward 5'-GTT GAC GGA CCC CAA AAG-3' and reverse 5'-GTG CTG CTG CGA GAT TTG-3', 93 bp; IL-1 α , forward 5'-TCA ACC AAA CTA TAT ATC AGG ATG TGG-3' and reverse 5'-CGA GTA GGC ATA CAT GTC AAA TTT TAC-3', 102 bp; IL-1RN, forward 5'-AAC CAC CAG GGC ATC ACA TA-3' and reverse 5'-CCT CTT GCC GAC ATG GAA TA-3', 150 bp; IL-1R1, forward 5'-GAG TTA CCC GAG GTC CAG-3' and reverse 5'-GAA GAA GCT CAC GTT GTC-3', 66 bp; TGF- β , forward 5'-ATA CGC CTG AGT GGC TGT C-3' and reverse

5'-GCC CTG TAT TCC GTC TCC T-3', 77 bp; and GAPDH, forward 5'-AAC TTT GGC ATT GTG GAA GG-3' and reverse 5'-GTC TTC TGG GTG GCA GTG AT-3', 62 bp [8].

Statistical analysis

The normality of the data (Kolmogorov–Smirnov test with Lilliefors' correction) and the homogeneity of variances (Levene median test) were tested. If both conditions were satisfied, differences between the groups were assessed by two-way ANOVA followed by Tukey's test. The comparison between the SIL and SIL-Cell groups was performed using the Student *t*-test or Mann–Whitney *U*-test for parametric and non-parametric data, respectively. Data are presented as the mean±standard error of the mean or median (25th to 75th percentiles) as appropriate. In all tests the significance level was set at 5%. Statistical analyses were done using SigmaStat 3.1 (Jandel Scientific, San Rafael, CA, USA).

RESULTS

BMDMC effects on survival, lung inflammation, and collagen accumulation

The pool of BMDMC intravenously injected were characterized by flow cytometry showing the following composition: total lymphocyte (4.18%) (CD45+, CD11b-, CD29-, CD34-), T lymphocyte (2.13%) (CD45+, CD3+, CD34-), T helper lymphocyte (0.47%) (CD4+, CD8-), T cytotoxic (1.66%) (CD4-, CD8+), monocytes (2.76%) (CD45+, CD29+, CD14+, CD38+, CD11b-, CD34- CD3-), granulocyte (78.7%) (CD45+, CD11b+, CD38+, CD34-, CD29-, CD14-, CD34- CD3-), hematopoietic progenitors (0.48%) (CD34+), and other progenitors (9.13%).

The animal survival rate was 100% in the C group and 53% in the SIL group. BMDMC injection yielded 79% survival rate ($p<0.05$).

Histological evaluation of the silica-treated mice showed interstitial and alveolar oedema, and granulomatous nodules with large accumulations of inflammatory cells. The treatment with BMDMC yielded a significant reduction in the area fraction of granuloma (144%) (fig. 1). However, no significant changes were observed in polymorphonuclear (PMN) and mononuclear (MN) cells in the granuloma. Conversely, silica-treated mice presented a higher number of PMN and MN cells in lung parenchyma compared with the C group. BMDMC therapy led to a reduction in PMN and MN cells (table 1).

In the SIL group, the number of BS-1-positive macrophages was increased in lung parenchyma and granuloma. BMDMC therapy resulted in a significant reduction of the amount of BS-1-positive macrophages in lung parenchyma with no significant changes in the granuloma (fig. 2).

The amount of collagen fibres in the alveolar septa and granuloma reduced after BMDMC therapy in silica-treated mice (fig. 3).

BMDMC effects on lung engraftment and IL-1 β , IL-1 α , IL-1RN, IL-1R1, TGF- β , and caspase-3

Y chromosome DNA was not detected in lung tissue at days 1, 3, 7 and 15 (see online supplementary material).

IL-1 β , IL-1 α , IL-1RN expressions were higher in SIL compared to C group (3.45-, 3.37-, and 4.40-fold, respectively) (fig. 4). BMDMC significantly reduced IL-1 β , IL-1 α , IL-1RN

mRNA expressions. IL-1R1 mRNA expression remained unaltered independent of silica or BMDMC administration.

Caspase-3 (fig. 5, *upper panel*) and TGF- β (*lower panel*) mRNA expressions in lung tissue were higher in SIL compared to C group (2.48- and 3.51-fold, respectively). BMDMC therapy significantly reduced caspase-3 and TGF- β mRNA expressions to control values.

Lung mechanics

There was no significant difference in flow and tidal volume among the groups. Static lung elastance ($E_{st,L}$), and lung resistive ($\Delta P_{1,L}$) and viscoelastic/inhomogeneous ($\Delta P_{2,L}$) pressures were similar in the C and C-Cell groups. In the SIL group, $E_{st,L}$, $\Delta P_{1,L}$ and $\Delta P_{2,L}$ were higher (177%, 150% and 177%, respectively) than in the C group. BMDMC significantly inhibited mechanical changes in the lung (fig. 6).

DISCUSSION

In the current study, we observed that early intravenous therapy with BMDMC led to a reduction in the area fraction of granuloma, the number of macrophages in the alveolar septa, and collagen fibre content resulting in an improvement in lung static elastance, viscoelastic and resistive pressures. These beneficial effects were shown to be not associated with engraftment but can be attributed to paracrine effects reducing caspase-3, IL-1 β , IL-1 α , IL-1RN, IL-1R1, and TGF- β mRNA expression.

Animal studies have shown that even a single exposure to crystalline silica can lead to pulmonary morpho-functional changes at day 15 mimicking the clinical setting [14-15]. Silica animals presented increased lung static elastance, viscoelastic and resistive pressures.

The changes observed in resistive pressure could be attributed to the intrabronchial cellular infiltration obstructing the lumen; the increase in lung static elastance and viscoelastic pressure may be associated with the presence of granulomatous nodules, increased number of cells in the alveolar septa and into the granuloma, and alveolar collapse, distortion of patent alveoli, and interstitial oedema, in accordance with previous studies on silica-treated BALB/c mice [14-16]. SIL group also showed an increase in the number of macrophages in the granuloma and lung parenchyma, which may release inflammatory cytokines, such as IL-1 [17], yielding a recruitment of inflammatory cells into the alveolar septa [17-18]. IL-1 family includes: IL-1 α , IL-1 β , and interleukin 1 receptor antagonist (IL-1RN), which bind to the same receptor, IL-1R1 [19-20]. In this context, the increase in levels of IL-1 expression in lung tissue was correlated with the development of pulmonary fibrosis. BMDMC therapy reduced IL-1 α and IL-1RN mRNA expressions in accordance with Ortiz et al. 2007 [19], who observed a decrease of IL-1 α and IL-1RN mRNA expressions after mesenchymal stem cell administration in a murine model of bleomycin-induced injury. Conversely, IL-1R1 mRNA expression remained unchanged after silica and/or BMDMC injection. Concurrent to the inflammatory process, the exposure to silica also initiates apoptosis [18, 21], increasing caspase-3 expression (fig. 4) [22]. Apoptosis has also been implicated in the trigger of the remodelling process [23], increasing TGF- β expression (fig. 4), which can influence mesenchymal cell migration, proliferation and extracellular matrix deposition [23-24]. Therefore, collagen fibre content increased in alveolar septa and granuloma (fig. 3). BMDMC reduced the inflammatory process decreasing the number of macrophages, which have a critical role in silica-induced lung fibrosis, and reducing IL-1 β expression in lung tissue. The reduction of IL-1 β mRNA expression may be related to

the decrease in the number of macrophages in lung parenchyma [2]. Pro-inflammatory cytokines, such as IL-1 β , play a key role in the development of silicosis by regulating the mediators that are responsible for the persistence of inflammation and development of fibrosis [25]. In addition, IL-1 β has been implicated in the deposition of collagen [26]. In this context, BMDMC reduced the amount of collagen fibre in the alveolar septa and granuloma, and TGF- β mRNA expression. Furthermore, apoptotic mechanisms have been implicated in silica-induced pathogenesis [2, 14, 16]. Caspase-3 expression was reduced in treated mice.

Previous studies have suggested that BMDCs have therapeutic potential for lung fibrosis [5-6]. These studies used mesenchymal stem cells (MSC), which require cell-culture processes yielding some disadvantages related to culture conditions detrimental for cell transplantation and the risk of contamination and immunological reactions [27]. Recently, hematopoietic stem cells have been recognized as progenitors for several cell types (endothelial, epithelial, myocytes and neurons) and able to reduce lung injury in murine model of fibrosis [28]. Therefore, in the present study bone marrow mononuclear cells, which are known to contain both hematopoietic and mesenchymal stem cells, were chosen to treat silica-induced lung fibrosis. Furthermore, the majority of stem cells are trapped inside the lungs following intravenous infusion, with BMDMC passage increased 30-fold compared with MSCs [29].

In a previous study, Ortiz and colleagues showed that mesenchymal stem cell therapy decreased lung inflammation and the levels of hydroxyproline in bleomycin-induced fibrosis [5]. Rojas et al. have also described a reduction in the expression of some

cytokines (IL-1 β , IL-2, and IL-4) and the repair of bleomycin-injured lungs [6]. Spees and colleagues, in a murine model of asbestos-induced pulmonary fibrosis, were able to identify rare bone marrow-derived cells with the phenotype of type II pneumocytes [7]. All these studies described an engraftment lower than 5% [5-6]. In this context, Lassance et al. reported that intratracheal instillation of BMDCs improved lung mechanics and histology independent of the ability of cells to engraft in the lung in a murine model of silicosis [8]. In silicotic animals, the use of fluorescent techniques to evaluate homing, such as green fluorescent protein positive cells and fluorescence in situ hybridization (FISH) analysis, is not feasible because silica crystal is highly birefringent. Therefore, in the present study, male DNA amplification by real-time PCR was carried out [5-6], and donor cells could not be detected in treated mice at days 1, 3, 7 and 15. The decrease in lung fibrosis by BMDMC therapy shown here could be ascribed to paracrine effects reducing the release of inflammatory and fibrogenic mediators.

In conclusion, the beneficial effects of early intravenous BMDMC therapy may be independent of bone marrow cell homing into the lung, but mediated through a down-regulation of inflammatory and fibrogenic responses to silica. Therefore, collagen fibre content was reduced followed by a reorganization of lung parenchyma and improvement in pulmonary mechanics. These findings are the first evidence that early administration of BMDMC therapy may have beneficial effects after silica-induced lung injury. Therefore, the present experimental model system could be used as starting point for more focused research in the future.

ACKNOWLEDGEMENTS

Supported by: Centers of Excellence Program (PRONEX-FAPERJ), Brazilian Council for Scientific and Technological Development (CNPq), Carlos Chagas Filho Rio de Janeiro State Research Supporting Foundation (FAPERJ), and Coordination for the Improvement of Higher Education Personnel (CAPES).

REFERENCES

1. Greenberg MI, Waksman J, Curtis J. Silicosis: a review. *Dis Mon* 2007: 53(8): 394-416.
2. Srivastava KD, Rom WN, Jagirdar J, Yie TA, Gordon T, Tchou-Wong KM. Crucial role of interleukin-1beta and nitric oxide synthase in silica-induced inflammation and apoptosis in mice. *Am J Respir Crit Care Med* 2002: 165(4): 527-533.
3. Hunninghake GW, Kalica AR. Approaches to the treatment of pulmonary fibrosis. *Am J Respir Crit Care Med* 1995: 151(3 Pt 1): 915-918.
4. Prockop DJ, Gregory CA, Spees JL. One strategy for cell and gene therapy: harnessing the power of adult stem cells to repair tissues. *Proc Natl Acad Sci U S A* 2003: 100 Suppl 1: 11917-11923.
5. Ortiz LA, Gambelli F, McBride C, Gaupp D, Baddoo M, Kaminski N, Phinney DG. Mesenchymal stem cell engraftment in lung is enhanced in response to bleomycin exposure and ameliorates its fibrotic effects. *Proc Natl Acad Sci U S A* 2003: 100(14): 8407-8411.
6. Rojas M, Xu J, Woods CR, Mora AL, Spears W, Roman J, Brigham KL. Bone marrow-derived mesenchymal stem cells in repair of the injured lung. *Am J Respir Cell Mol Biol* 2005: 33(2): 145-152.
7. Spees JL, Pociask DA, Sullivan DE, Whitney MJ, Lasky JA, Prockop DJ, Brody AR. Engraftment of bone marrow progenitor cells in a rat model of asbestos-induced pulmonary fibrosis. *Am J Respir Crit Care Med* 2007: 176(4): 385-394.
8. Lassance RM, Prota LF, Maron-Gutierrez T, Garcia CS, Abreu SC, Passaro CP, Xisto DG, Castiglione RC, Carreira HJ, Santana MC, Souza SA, Gutfilen B, Fonseca LM, Rocco PR, Morales MM. Intratracheal instillation of bone marrow-derived cell in an experimental model of silicosis. *Respir Physiol Neurobiol* 2009.
9. Bates JH, Decramer M, Chartrand D, Zin WA, Boddener A, Milic-Emili J. Volume-time profile during relaxed expiration in the normal dog. *J Appl Physiol* 1985: 59(3): 732-737.

10. Weibel ER. Morphometry: stereological theory and practical methods. *In*: Dekker GJNY, ed. Models of Lung Disease-Microscopy and Structural Methods, 1990; pp. 199-247.
11. Montes GS. Structural biology of the fibres of the collagenous and elastic systems. *Cell Biol Int* 1996; 20(1): 15-27.
12. Baleeiro CE, Christensen PJ, Morris SB, Mendez MP, Wilcoxon SE, Paine R, 3rd. GM-CSF and the impaired pulmonary innate immune response following hyperoxic stress. *Am J Physiol Lung Cell Mol Physiol* 2006; 291(6): L1246-1255.
13. Maddox DE, Shibata S, Goldstein IJ. Stimulated macrophages express a new glycoprotein receptor reactive with Griffonia simplicifolia I-B4 isolectin. *Proc Natl Acad Sci U S A* 1982; 79(1): 166-170.
14. Borges VM, Falcao H, Leite-Junior JH, Alvim L, Teixeira GP, Russo M, Nobrega AF, Lopes MF, Rocco PM, Davidson WF, Linden R, Yagita H, Zin WA, DosReis GA. Fas ligand triggers pulmonary silicosis. *J Exp Med* 2001; 194(2): 155-164.
15. Faffe DS, Silva GH, Kurtz PM, Negri EM, Capelozzi VL, Rocco PR, Zin WA. Lung tissue mechanics and extracellular matrix composition in a murine model of silicosis. *J Appl Physiol* 2001; 90(4): 1400-1406.
16. Borges VM, Lopes MF, Falcao H, Leite-Junior JH, Rocco PR, Davidson WF, Linden R, Zin WA, DosReis GA. Apoptosis underlies immunopathogenic mechanisms in acute silicosis. *Am J Respir Cell Mol Biol* 2002; 27(1): 78-84.
17. Rimal B, Greenberg AK, Rom WN. Basic pathogenetic mechanisms in silicosis: current understanding. *Curr Opin Pulm Med* 2005; 11(2): 169-173.
18. Huaux F. New developments in the understanding of immunology in silicosis. *Curr Opin Allergy Clin Immunol* 2007; 7(2): 168-173.
19. Ortiz LA, Dutreil M, Fattman C, Pandey AC, Torres G, Go K, Phinney DG. Interleukin 1 receptor antagonist mediates the antiinflammatory and antifibrotic effect of mesenchymal stem cells during lung injury. *Proc Natl Acad Sci U S A* 2007; 104(26): 11002-11007.

20. Sims JE, Smith DE. The IL-1 family: regulators of immunity. *Nat Rev Immunol* 2010; 10(2): 89-102.
21. Lalmanach G, Diot E, Godat E, Lecaille F, Herve-Grepinet V. Cysteine cathepsins and caspases in silicosis. *Biol Chem* 2006; 387(7): 863-870.
22. Shen HM, Zhang Z, Zhang QF, Ong CN. Reactive oxygen species and caspase activation mediate silica-induced apoptosis in alveolar macrophages. *Am J Physiol Lung Cell Mol Physiol* 2001; 280(1): L10-17.
23. Delgado L, Parra ER, Capelozzi VL. Apoptosis and extracellular matrix remodelling in human silicosis. *Histopathology* 2006; 49(3): 283-289.
24. Jagirdar J, Begin R, Dufresne A, Goswami S, Lee TC, Rom WN. Transforming growth factor-beta (TGF-beta) in silicosis. *Am J Respir Crit Care Med* 1996; 154(4 Pt 1): 1076-1081.
25. Barbarin V, Arras M, Misson P, Delos M, McGarry B, Phan SH, Lison D, Huaux F. Characterization of the effect of interleukin-10 on silica-induced lung fibrosis in mice. *Am J Respir Cell Mol Biol* 2004; 31(1): 78-85.
26. Zhang Y, Lee TC, Guillemin B, Yu MC, Rom WN. Enhanced IL-1 beta and tumor necrosis factor-alpha release and messenger RNA expression in macrophages from idiopathic pulmonary fibrosis or after asbestos exposure. *J Immunol* 1993; 150(9): 4188-4196.
27. Kumamoto M, Nishiwaki T, Matsuo N, Kimura H, Matsushima K. Minimally-cultured Bone Marrow mesenchymal stem cells ameliorate fibrotic lung injury. *Eur Respir J* 2009.
28. Aguilar S, Scotton CJ, McNulty K, Nye E, Stamp G, Laurent G, Bonnet D, Janes SM. Bone marrow stem cells expressing keratinocyte growth factor via an inducible lentivirus protects against bleomycin-induced pulmonary fibrosis. *PLoS ONE* 2009; 4(11): e8013.
29. Fischer UM, Harting MT, Jimenez F, Monzon-Posadas WO, Xue H, Savitz SI, Laine GA, Cox CS, Jr. Pulmonary passage is a major obstacle for intravenous stem cell delivery: the pulmonary first-pass effect. *Stem Cells Dev* 2009; 18(5): 683-692.

TABLE 1 Total and differential cellularity in lung parenchyma and granuloma

	PMN (%)	MN (%)
Lung parenchyma		
C	0.43±0.11	29.75±0.38
C-Cell	1.67±0.51	28.09±2.00
SIL	5.95±0.65*	35.02±0.71*
SIL-Cell	2.63±0.67	27.00±0.75
Granuloma		
SIL	8.35±0.81	28.36±0.65
SIL-Cell	7.57±1.05	27.91±2.14

C and SIL mice received saline (50 µl) or silica (20 mg silica/50 µl saline) intratracheally, respectively. C and SIL animals were treated with saline or BMDMC (2×10^6 i.v.). % MN, percentage of mononuclear cells, % PMN, percentage of polymorphonuclear cells. Values are means of 5 animals (±SEM) in each group. *Significantly different from C.

FIGURE LEGENDS

FIGURE 1. Photomicrographs of lung parenchyma stained with haematoxylin-eosin: (A) C; (B) C-Cell; (C) SIL; (D) SIL-Cell groups. Note the presence of granuloma in SIL animals (asterisk). Quantification of fraction area of granuloma (E). C and SIL mice received saline or silica intratracheally. C and SIL animals were treated with BMDMC (2×10^6 i.v., C-Cell and SIL-Cell, respectively). #Significantly different from SIL.

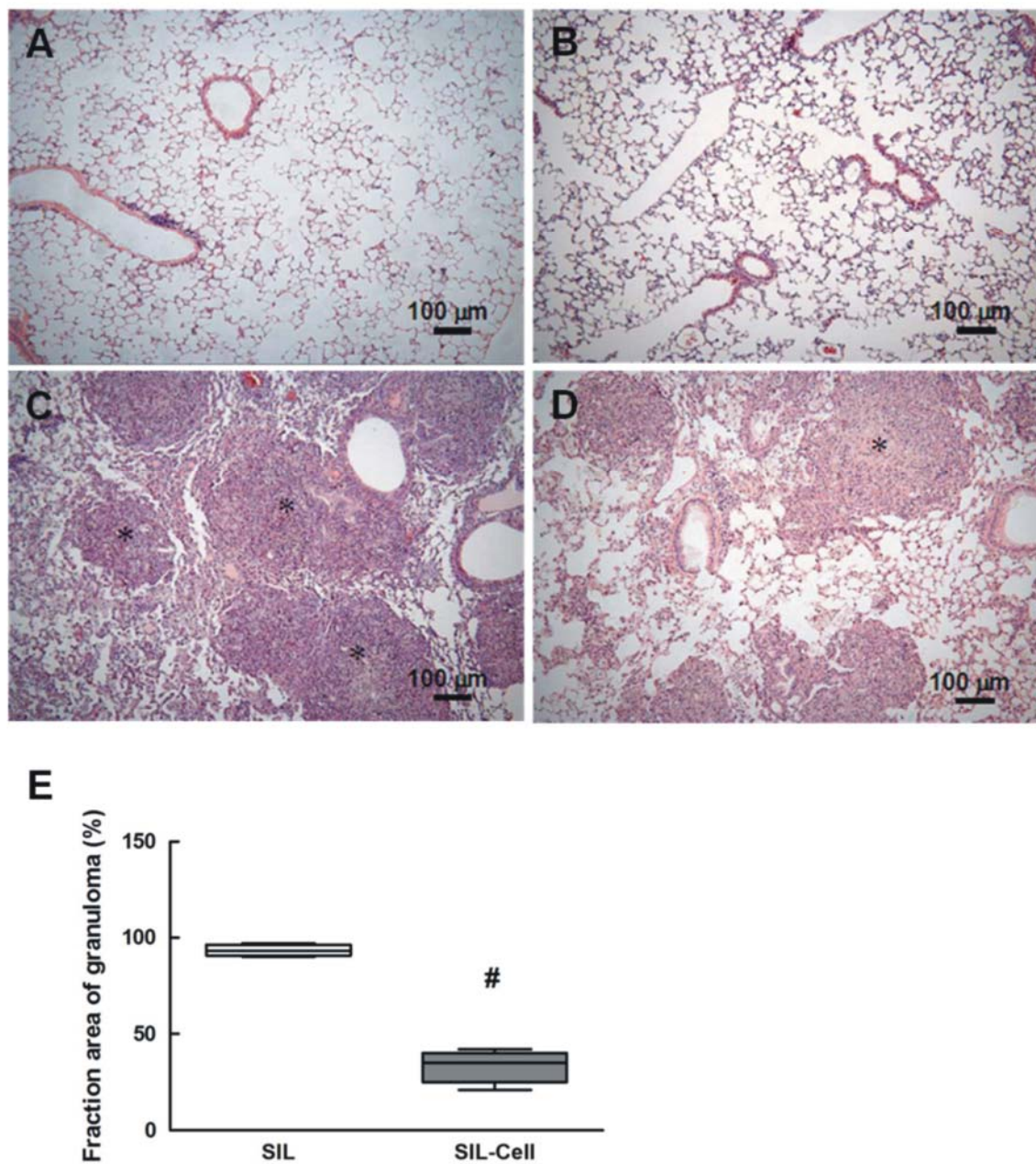


FIGURE 2. Photomicrographs of lung parenchyma after lectin histochemistry: (A) C; (B) C-Cell; (C) SIL; (D) SIL-Cell groups. Note the macrophages in lung parenchyma and in granuloma (arrows). Quantification of macrophages in lung parenchyma (E) and in the granuloma (F). C and SIL mice received saline or silica intratracheally. C and SIL animals

were treated with BMDMC (2×10^6 i.v., C-Cell and SIL-Cell, respectively). Values are means of 5 animals (\pm SEM) in each group. *Significantly different from C.

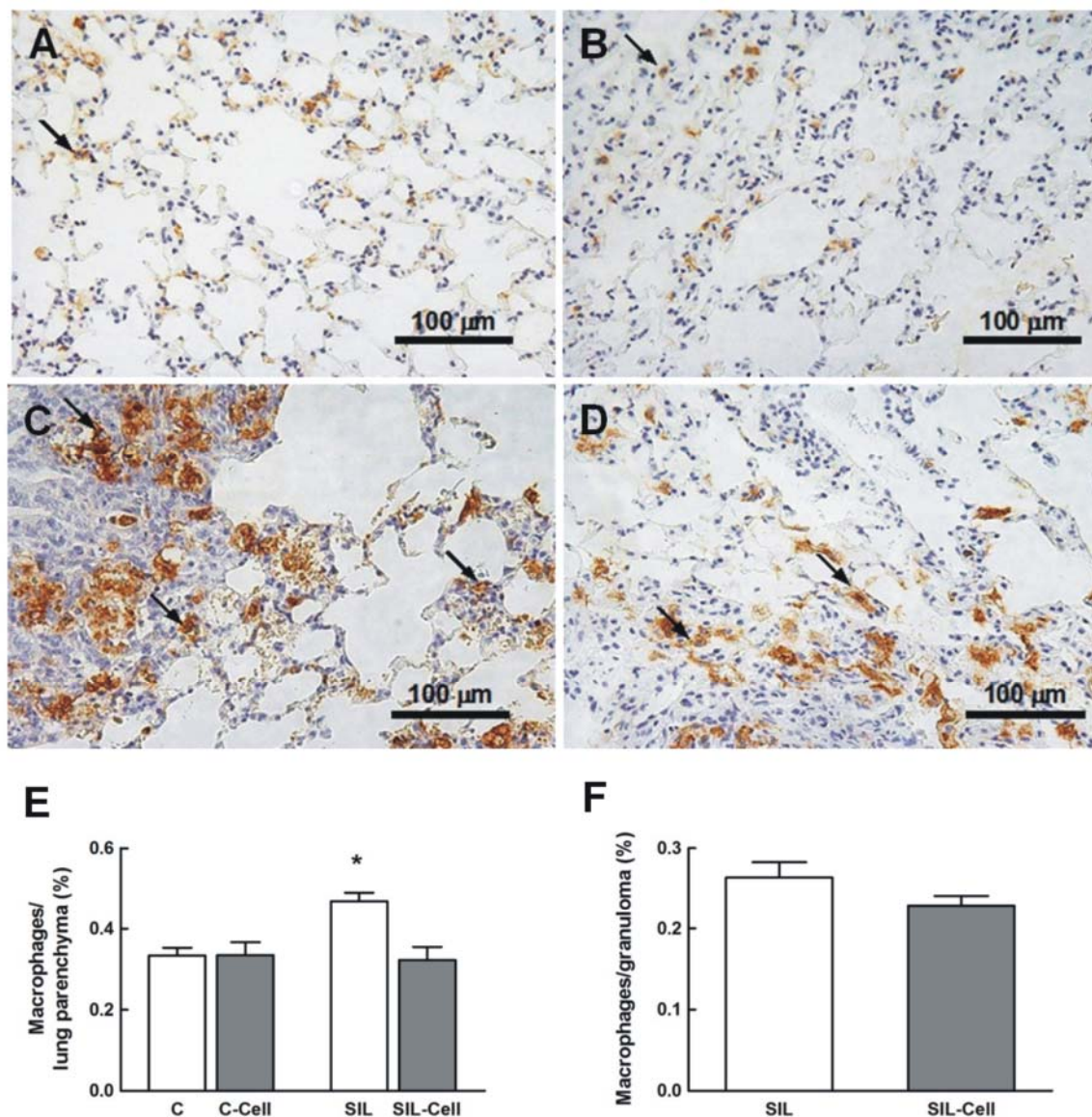


FIGURE 3. Photomicrographs of lung parenchyma stained with picosirius under polarization: (A) C; (B) C-Cell; (C) SIL; (D) SIL-Cell groups; and collagen fibre content in alveolar septa (E) and in the granuloma (F). C and SIL mice received saline or silica intratracheally. C and SIL animals were treated with BMDMC (2×10^6 i.v., C-Cell and SIL-

Cell, respectively). Values are means of 5 animals (\pm SEM) in each group. *Significantly different from C. #Significantly different from SIL.

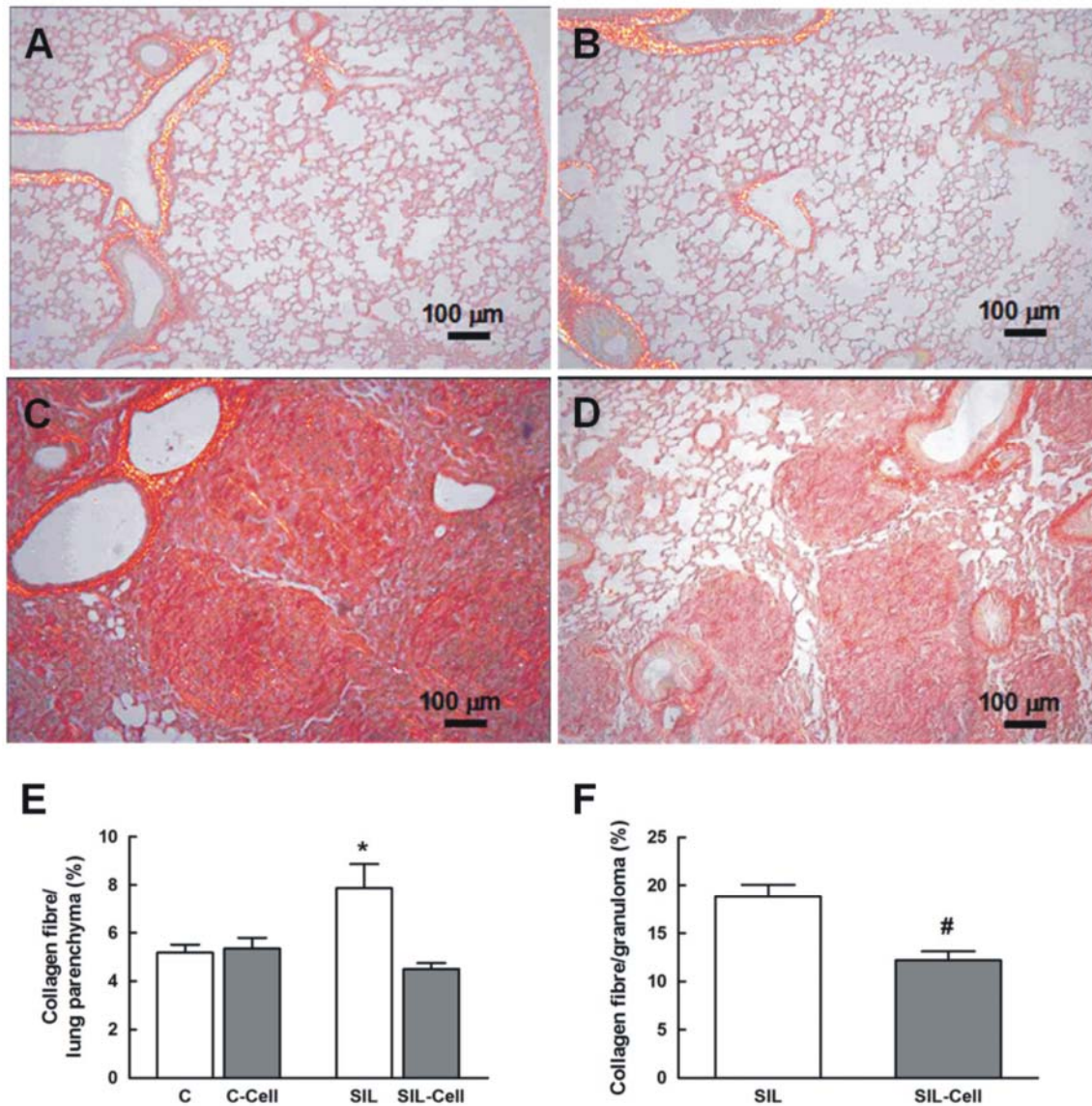


FIGURE 4. Real-time PCR analysis of IL-1 β , IL-1 α , interleukin-1 receptor antagonist (IL-1RN), interleukin-1 receptor type 1 (IL-1R1) mRNA expressions. C and SIL mice received saline or silica intratracheally. C and SIL animals were treated with BMDMC (2×10^6 i.v.,

C-Cell and SIL-Cell, respectively). Values are means of 5 animals (\pm SEM) in each group.

*Significantly different from C.

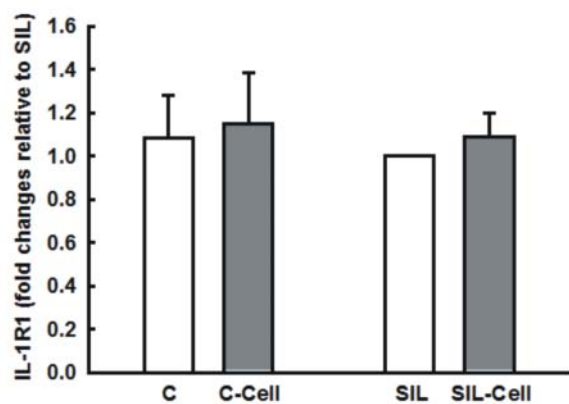
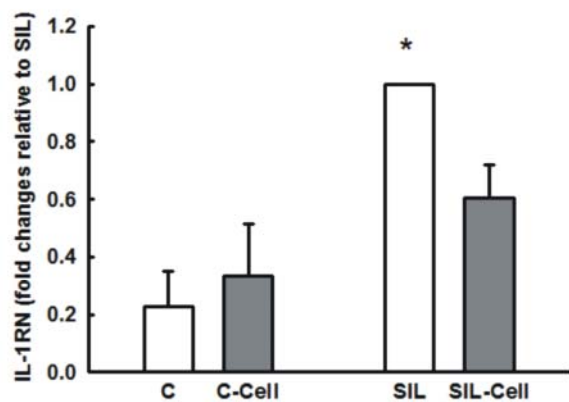
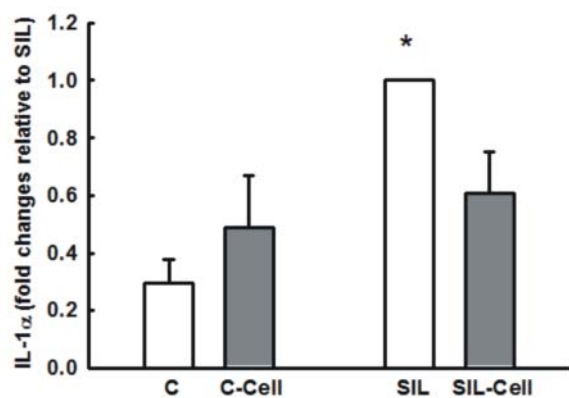
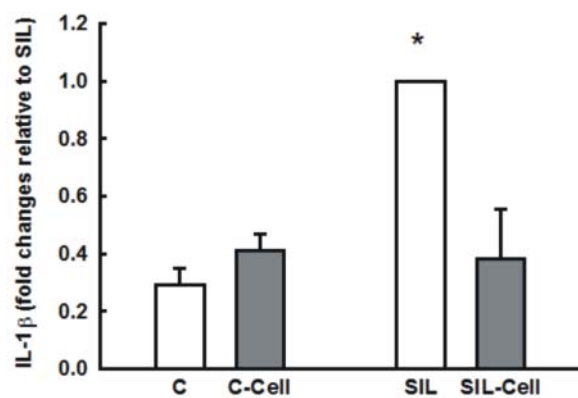


FIGURE 5. Real-time PCR analysis of caspase-3 and transforming growth factor (TGF)- β mRNA expressions. C and SIL mice received saline or silica intratracheally. C and SIL animals were treated with BMDMC (2×10^6 i.v., C-Cell and SIL-Cell, respectively). Values are means of 5 animals (\pm SEM) in each group. *Significantly different from C.

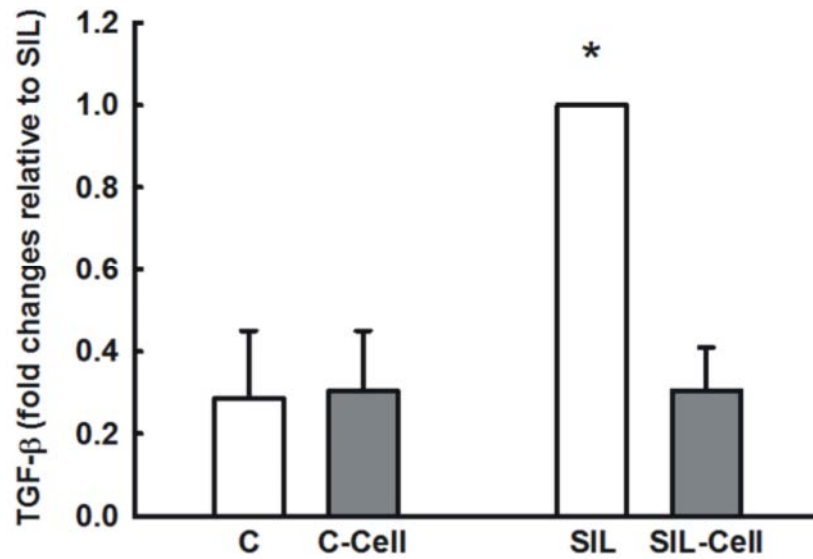
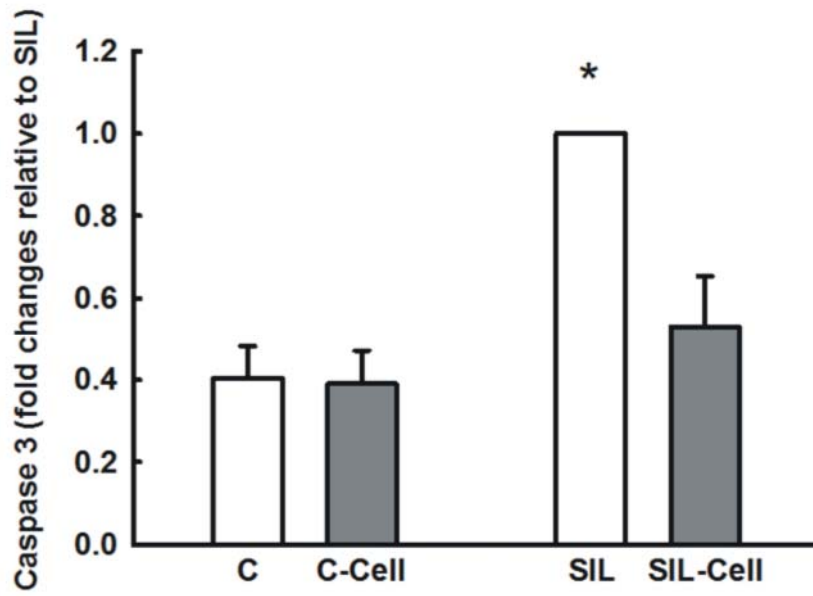


FIGURE 6. Lung static elastance (E_{st}), resistive pressure (ΔP_1) and viscoelastic/inhomogeneous (ΔP_2) pressure. C and SIL mice received saline or silica intratracheally. C and SIL animals were treated with BMDMC (2×10^6 i.v., C-Cell and SIL-

Cell, respectively). Values are means of 8 animals (\pm SEM) in each group. *Significantly different from C.

